


Our Reference: JMST 761

P-authorquery-v8

## AUTHOR QUERY FORM

 ELSEVIER	<b>Journal: JMST</b>  <b>Article Number: 761</b>	<b>Please e-mail your responses and any corrections to:</b>  <b>E-mail: <a href="mailto:corrections.esch@elsevier.toppanbestset.com">corrections.esch@elsevier.toppanbestset.com</a></b>
---	--	--

Dear Author,

Please check your proof carefully and mark all corrections at the appropriate place in the proof (e.g., by using on-screen annotation in the PDF file) or compile them in a separate list. To ensure fast publication of your paper please return your corrections within 48 hours.

For correction or revision of any artwork, please consult <http://www.elsevier.com/artworkinstructions>.

We were unable to process your file(s) fully electronically and have proceeded by

Scanning (parts of) your article       Rekeying (parts of) your article       Scanning the artwork

Any queries or remarks that have arisen during the processing of your manuscript are listed below and highlighted by flags in the proof. Click on the '[Q](#)' link to go to the location in the proof.

Location in article	Query / Remark: <a href="#">click on the Q link to go</a> Please insert your reply or correction at the corresponding line in the proof
<a href="#">Q1</a>	Please confirm that given names and surnames have been identified correctly and are presented in the desired order.
<a href="#">Q2</a>	Your article is registered as a regular item and is being processed for inclusion in a regular issue of the journal. If this is NOT correct and your article belongs to a Special Issue/ Collection please contact < <a href="mailto:l.ashwin@elsevier.com">l.ashwin@elsevier.com</a> > immediately prior to returning your corrections.
<a href="#">Q3</a>	'As a result. . .': This sentence has been reworded for clarity. Please check that the meaning is still correct.
<a href="#">Q4</a>	Is 'objects linkage' changed to 'object linkages' correct?
<a href="#">Q5</a>	Please check if changes made to structures marked by '-' (bond rule) and '=' (double bond rule) are correct.
<a href="#">Q6</a>	Is changing from 'FTIR spectrum of pyrolyzed to 400 °C hybrid precursor' to 'FTIR spectrum <b>of PVA/B<sub>2</sub>O<sub>3</sub></b> pyrolyzed to 400 °C hybrid precursor' correct? Please amend the text if necessary.
<a href="#">Q7</a>	Is changing from 'IR spectra of pyrolyzed to 400 °C hybrid precursor' to 'IR spectra <b>of PVA/PEG/B<sub>2</sub>O<sub>3</sub></b> pyrolyzed to 400 °C hybrid precursor' correct? Please amend the text if necessary.
<a href="#">Q8</a>	Is changing from 'IR studies of pyrolyzed to. . .' to 'IR studies <b>of PVA/PEG/B<sub>2</sub>O<sub>3</sub></b> pyrolyzed to. . .' correct? Please amend the text if necessary.
<a href="#">Q9</a>	'The other three groups. . .': This sentence has been reworded for clarity. Please check that the meaning is still correct.
<a href="#">Q10</a>	Please clarify which do you mean: ' <b>independent of</b> specific experimental conditions' or ' <b>dependent on</b> specific experimental conditions'? Please amend text if necessary.
<a href="#">Q11</a>	The references should be sequentially cited in the text, hence refs have been renumbered both in the text and in the reference list from Ref. 27 onwards. Please check, and correct if necessary.
<a href="#">Q12</a>	Please provide abbreviated journal titles for Reference Fathi et al., 2012.

Thank you for your assistance.

<a href="#">Q13</a>	<p>This section comprises references that occur in the reference list but not in the body of the text. Please position this reference in the text or, alternatively, delete it. Any reference not dealt with will be retained in this section. Thank you.</p> <table border="1" data-bbox="504 342 1259 414"><tr><td data-bbox="504 342 1161 414">Please check this box or indicate your approval if you have no corrections to make to the PDF file</td><td data-bbox="1161 342 1259 414"><input type="checkbox"/></td></tr></table>	Please check this box or indicate your approval if you have no corrections to make to the PDF file	<input type="checkbox"/>
Please check this box or indicate your approval if you have no corrections to make to the PDF file	<input type="checkbox"/>		



Contents lists available at ScienceDirect

## Journal of Materials Science &amp; Technology

journal homepage: [www.jmst.org](http://www.jmst.org)

## Boron Oxide Glasses and Nanocomposites: Synthetic, Structural and Statistical Approach

Hristo Hristov<sup>1</sup>, Miroslava Nedialkova<sup>1,\*</sup>, Sergio Madurga<sup>2</sup>, Vasil Simeonov<sup>1</sup>

<sup>1</sup> Faculty of Chemistry and Pharmacy, University of Sofia, Sofia 1164, Bulgaria

<sup>2</sup> Physical Chemistry Department and Research Institute of Theoretical and Computational Chemistry (IQTUCB) of the University of Barcelona (UB), Barcelona 08028, Catalonia, Spain

## ARTICLE INFO

## Article history:

Received 27 February 2016

Received in revised form

30 March 2016

Accepted 1 April 2016

Available online

## Key words:

Organic-inorganic hybrid materials

Borate glass

Nanocomposites

Cluster analysis

Three different precursors of boron-aqua and glycerol solutions of boric acid and ethanol solution of trimethyl borate were used for the preparation of organic-inorganic advanced materials. The films and bulk materials samples were heat treated at 100, 400, 800 °C for 2 h. The hybrid samples were stable and transparent until 100 °C. The further increase of temperature to 400 °C led to destruction of samples, and at 800 °C they were molten. The structural changes during the pyrolysis were studied by Fourier transform infrared spectroscopy, differential thermal analysis, and X-ray diffraction. Details of surface morphology were observed by scanning electron microscopy. The obtained BO<sub>3</sub> and BO<sub>4</sub> groups were identified in the molten materials after pyrolysis. The quantities and order of borate structural units as well as residual carbon in the networks depended on boron precursor type. PVA/PEG/B<sub>2</sub>O<sub>3</sub> hybrid materials were proved to be appropriate precursors for synthesizing borate and carboborate glass and carbon/borate glass nanocomposites. To access the impact of the experimental conditions on the structural changes of the nanocomposites, cluster analysis of the IR-spectral data was used as a classification method.

Copyright © 2016, The editorial office of Journal of Materials Science & Technology. Published by Elsevier Limited.

### 1. Introduction

Pure borate glass is made up of a random network including boroxol rings (B<sub>3</sub>O<sub>6</sub>) and threefold coordinate boron (BO<sub>3</sub>). The addition of modifiers, such as alkaline, supports the formation of BO<sub>4</sub> groups in the glass structure. The structuring role of the network modifier is determined by its size, charge and network forming agent of the glass. Through sol-gel processing, homogeneous, high-purity inorganic oxide glasses can be made at ambient temperatures rather than at very high temperatures as required in conventional approaches. The sol-gel process is a useful technique for processing a large number of technologically important glasses, glass-ceramics and crystalline ceramics, mainly because of its ability to generate stoichiometric materials with good control over final amount of compositions.

Significantly, less number of borate compositions is modified by low-temperature sol-gel technology. Special attention has been given to the effect of the ionic conductivity of alkali-borate glasses, especially of lithium-borate, and possibility of applications for solid state batteries and energy storage devices<sup>[1-3]</sup>. The hybrid borate

hydrogel materials obtained by sol-gel technology with a combination of aqua soluble polymers, like polyvinyl alcohol (PVA) and polyethylene glycol (PEG), may have potential applications. Such materials are hybrids of borate esters applied as an electrolyte in lithium-ion batteries<sup>[4-8]</sup> and materials for medical and biotechnological applications<sup>[9-11]</sup>. Incorporations of boron in the polymer backbone are used for reinforcing carbon/carbon composite materials. As a result, carbon active sites are blocked because boron generates an oxygen diffusion barrier on the surface of the materials, preventing oxygen from reaching the carbon surface<sup>[12-15]</sup>. Ceramic fiber<sup>[16]</sup>, boron carbide<sup>[17-20]</sup> and boron nitride ceramics<sup>[21]</sup> are produced using only PVA-B<sub>2</sub>O<sub>3</sub> hybrid precursors. For borate glasses, data exist only for the cases of metal counterions for anions borate units' compensation. In this work, PVA/PEG/B<sub>2</sub>O<sub>3</sub> precursors for boron doped carbon, materials are provided. The polymer pyrolysis is a simple processing route to produce multicomponent nanostructured materials. According to this method, organic-inorganic materials are converted to the borate and carboborate glass and carbon/borate glass nanocomposites.

The objective of the present study is to probe the structure of the hybrid borate hydrogel materials. The crosslinking is achieved by a combination of PVA and PEG in different solutions of borate species. The study is relevant because the new findings will provide information about the basic units forming this multicomponent glass

\* Corresponding author.

E-mail address: [mici345@yahoo.com](mailto:mici345@yahoo.com) (M. Nedialkova).

structure. Additionally, multivariate statistical interpretation of infrared spectral data (hierarchical cluster analysis) was used to determine specific experimental conditions impacting the procedure of synthesis.

## 2. Experimental

By the sol-gel process at ambient temperature, homogeneous and transparent organic-inorganic gel materials were obtained with PVA/PEG/B<sub>2</sub>O<sub>3</sub> mass ratio of 10/7/1 by the method referred to in the literature<sup>[22-24]</sup>. All chemicals were used without any further purification: polyvinyl alcohol 72000 (PVA) 98% hydrolyzed, polyethylene glycol 400 (PEG), trimethyl borate (CH<sub>3</sub>O)<sub>3</sub>B, boric acid (H<sub>3</sub>BO<sub>3</sub>) from Sigma-Aldrich Chemie, Germany. A stock solution of 4 wt% PVA was prepared by dissolving PVA in distilled water by heating. Three precursor solutions of boron are used: 4 wt% H<sub>3</sub>BO<sub>3</sub> in distilled water, 4 wt% H<sub>3</sub>BO<sub>3</sub> prepared in glycerol and 4 wt% (CH<sub>3</sub>O)<sub>3</sub>B in ethanol.

The hybrid gels were made by initially mixing and homogenizing PEG and different stock boron solutions. After that, the blended solution was added to the PVA under constant stirring. To obtain self-standing films, and bulk material samples, the hybrid gels were cast onto a glass plate or in a beaker for producing two types of samples for the next steps. The obtained films with 40 μm in thickness and bulk material samples were dried at ambient temperature for one week. The next phase in the experimental procedure was heat treatment at 100, 400, 800 °C for 2 h. Structural changes during the pyrolysis were studied by Fourier transform infrared spectroscopy (FTIR, Perkin Elmer SPECTRUM 1000), differential thermal analysis (TG/DTA, SETRAM LABYS TG/DTA), X-ray diffraction (XRD, DRON-UN CuK<sub>α</sub>). The surface morphology was observed by scanning electron microscopy (SEM, JEOL JSM 5300).

Cluster analysis (CA) is a well-known and widely used data mining approach for various purposes with its hierarchical and non-hierarchical algorithms<sup>[25,26]</sup>. Experimental samples (objects) could be characterized by a set of variables and cluster analysis allows to determine their similarity and to define cluster objects both for objects and variables. A preliminary step of data scaling is necessary (auto scaling or z-transform) for normalized dimensionless numbers replacing the real data values. Thus, important differences in absolute values could be reduced to close numbers. Then, the similarity (or more strictly, the distance) between the objects in the variable space has to be determined. Very often the Euclidean distance was used for clustering purposes. Another approach of measuring similarity is the calculation of the correlation coefficient between the objects. Thus, from the input matrix (raw data) a similarity matrix could be constructed. There is a wide variety of hierarchical algorithms of object linkages, but the typical ones include the single linkage, the complete linkage, and the average linkage methods. The Ward's linkage method was used. The representation of the results of the cluster analysis was performed by a tree-like scheme called dendrogram comprising a hierarchical structure (large groups are divided into small ones).

## 3. Results and Discussion

### 3.1. FTIR spectra

All obtained hybrid materials were transparent and thermally stable up to 100 °C, and over 400 °C they were converted into black powder. The final pyrolyzed products were obtained at 800 °C as transparent borate glasses, or black melt carbon/borate glass nanocomposites. Structural changes, which are visually observed, were gained as a function of the borate solutions type. Figs. 1-4 show the FTIR spectra for hybrid precursors during pyrolysis for PVA/PEG/B<sub>2</sub>O<sub>3</sub>.

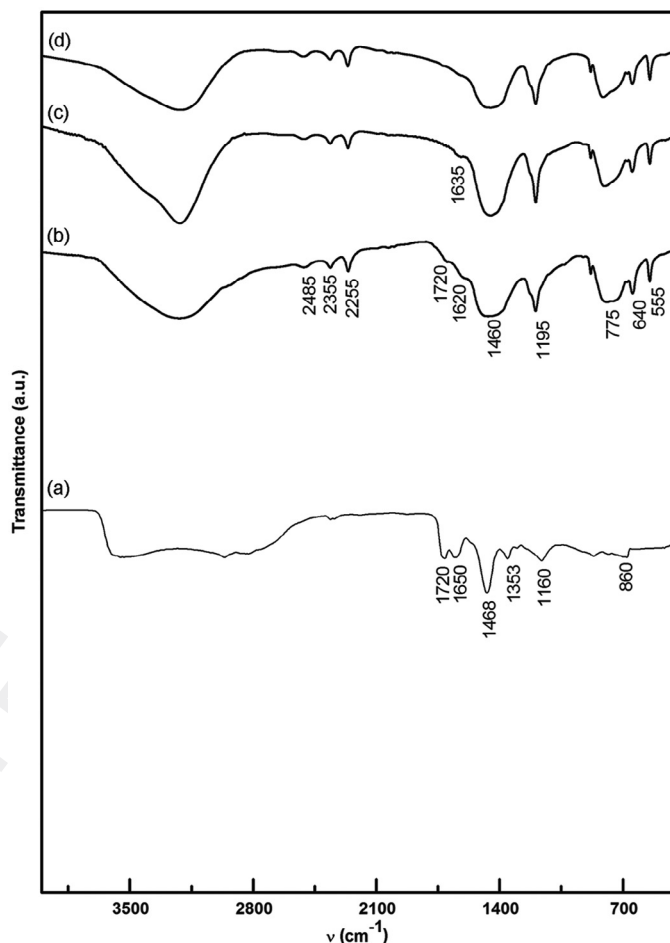
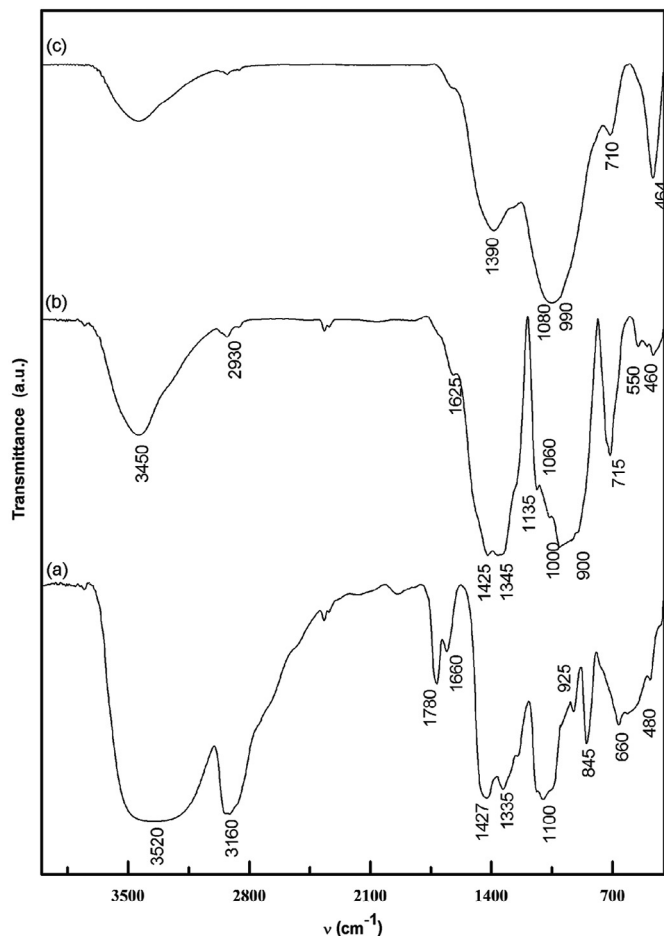


Fig. 1. Fourier transform infrared (FTIR) spectra (spectra are vertically shifted) of pyrolyzed hybrid precursor PVA/B<sub>2</sub>O<sub>3</sub>: (a) 100 °C, (b) 400 °C, (c) 800 °C, (d) H<sub>3</sub>BO<sub>3</sub> molten of 800 °C.

The absorption bands presented at 100 °C are assigned to: 3700-3100 cm<sup>-1</sup> (ν<sub>s</sub>H-OH, ν<sub>s</sub>C-OH, ν<sub>s</sub>B-OH, hydrogen bonds), 2940-2870 cm<sup>-1</sup> (ν<sub>s</sub>C-H of CH<sub>2</sub>, CH<sub>3</sub>), 2300-1900 cm<sup>-1</sup> (δ hydrogen bonds), 1720-1710 cm<sup>-1</sup> (ν<sub>s</sub>C=O), 1650-1640 cm<sup>-1</sup> (O-H of H<sub>2</sub>O, C-C), 1460-1425 cm<sup>-1</sup> (ν<sub>as</sub>O-H, δ<sub>C</sub>-H of CH<sub>2</sub> and C-C), 1370-1350 cm<sup>-1</sup> (δ<sub>as</sub>CH<sub>3</sub> and C-C), 1370-1220 cm<sup>-1</sup> (δ<sub>C</sub>-OH, ν<sub>O</sub>-C-C), 1120-1080 cm<sup>-1</sup> (ν<sub>C</sub>-OH of secondary alcohol PVA, Glycerol), 1065-1020 cm<sup>-1</sup> (ν<sub>C</sub>-OH of primary alcohol PEG, Glycerol), 1100-1000 cm<sup>-1</sup> (δ<sub>C</sub>-O-C of esters), 1200-970 cm<sup>-1</sup> (δ<sub>C</sub>-O), 940-920 cm<sup>-1</sup> (γ<sub>C</sub>-OH and δ<sub>C</sub>-C), 700-670 cm<sup>-1</sup> (δ<sub>C</sub>-H and C-C)<sup>[16-21,27,28]</sup>. The bands in region 1500-1200 cm<sup>-1</sup> are allied to (ν<sub>B</sub>-O of BO<sub>3</sub>), 1200-850 cm<sup>-1</sup> to (ν<sub>B</sub>-O of BO<sub>4</sub>) and 800-600 cm<sup>-1</sup> (bending vibrations for various borate segments)<sup>[29,30]</sup>. The characteristic frequency for B-O-C bond occurred at 1030 cm<sup>-1</sup><sup>[16-19]</sup>.

The major changes of vibration frequencies for O-H and C-OH (3700-3100 cm<sup>-1</sup>) and C-H (2940-2870 cm<sup>-1</sup>) bonds are observed in FTIR spectra at 400 °C. The effects of water evaporation and burning of polymers lead to decrease of widths and intensities of these bands<sup>[31]</sup>. The spectral changes depicted in Figs. 1 and 2 are connected to the simultaneous disappearance of the absorptions bands in the regions of 2940-2870 cm<sup>-1</sup> and 1720 cm<sup>-1</sup>. The presence of new bands at 700 cm<sup>-1</sup>, 460 cm<sup>-1</sup>, 550 cm<sup>-1</sup> indicates the presence of BO<sub>3</sub> groups<sup>[16,19,29,30]</sup>. The network of the PVA-H<sub>3</sub>BO<sub>3</sub> hybrid precursor at 400 °C is destroyed, and typical bands of BO<sub>3</sub> group in boric acid are observed in Fig. 1(b). FTIR spectrum of PVA/B<sub>2</sub>O<sub>3</sub>



**Fig. 2.** Fourier transform infrared (FTIR) spectra (spectra are vertically shifted) of pyrolyzed PVA/PEG/B<sub>2</sub>O<sub>3</sub> hybrid precursor, prepared from glycerol solution of H<sub>3</sub>BO<sub>3</sub>: (a) 100 °C, (b) 400 °C, (c) 800 °C.

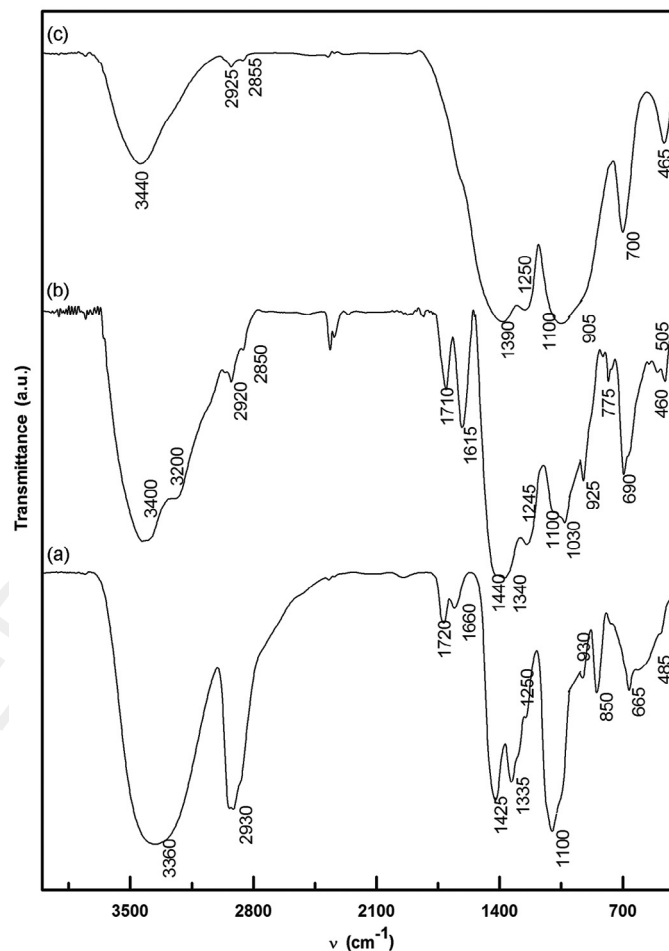


**Fig. 3.** Fourier transform infrared (FTIR) spectra (spectra are vertically shifted) of pyrolyzed PVA/PEG/B<sub>2</sub>O<sub>3</sub> hybrid precursor, prepared from aqueous solution of H<sub>3</sub>BO<sub>3</sub>: (a) 100 °C, (b) 400 °C, (c) 800 °C.

pyrolyzed to 400 °C hybrid precursor produced by a glycerol solution of boric acid is presented in Fig. 2(b). The bands intensities are increased in regions of 1425–1345 cm<sup>-1</sup> (BO<sub>3</sub>) and 1060–900 cm<sup>-1</sup> (BO<sub>4</sub>). These can be linked to the rearrangement of initially cross-linked borate groups. Figs. 3 and 4 show the IR spectra of PVA/PEG/B<sub>2</sub>O<sub>3</sub> pyrolyzed to 400 °C hybrid precursor prepared by an aqueous solution of boric acid and ethanol solution of boron methoxide. The observed changes resulted from the increase in frequency intensities at wavenumber ranges of 1400–1200 cm<sup>-1</sup> (BO<sub>3</sub>) and 1100–900 cm<sup>-1</sup> (BO<sub>4</sub>). The IR spectra revealed a diminishing trend of the BO<sub>4</sub>/BO<sub>3</sub> ratio. The occurrence of new bands 1030 cm<sup>-1</sup> and 800 cm<sup>-1</sup> can be assigned to B–O–C bonds and BO<sub>4</sub> groups, respectively, while the absorptions bands at 1200 cm<sup>-1</sup>, 700 cm<sup>-1</sup>, 645 cm<sup>-1</sup>, 550 cm<sup>-1</sup> are typical of boric acid in Fig. 4(b). The changes of absorption bands at wavenumber regions of 3200–2900 cm<sup>-1</sup>, 1700–1400 cm<sup>-1</sup>, 1000–600 cm<sup>-1</sup> can be assigned according to the vibrations frequencies of unsaturated hydrocarbons<sup>[32,33]</sup> to 3100–3000 cm<sup>-1</sup> (ν<sub>s</sub>C–H), 1730–1700 cm<sup>-1</sup> (ν<sub>s</sub>C=O of aldehydes and ketones), 1680–1600 cm<sup>-1</sup> (ν<sub>s</sub>C=C), 1400 cm<sup>-1</sup> (δ = C–H), 1000–600 cm<sup>-1</sup> (δ = C–H). The observed structural changes for all samples at 400–800 °C show two opposite tendencies: the simultaneous decomposition of hybrid networks and polymerization of BO<sub>3</sub> and BO<sub>4</sub> in borate glass networks. From IR analysis, it can be concluded that thermal stability of PVA–B<sub>2</sub>O<sub>3</sub> hybrid precursor is the lowest one. The IR spectrum at 800 °C corresponds to molten H<sub>3</sub>BO<sub>3</sub> shown in Fig. 1(c,d) and

no structural changes occur compared to that at 400 °C. The final product is transparent borate glass, containing only BO<sub>3</sub> groups. Regarding the three component systems, the hybrid PVA/PEG/B<sub>2</sub>O<sub>3</sub> precursor prepared by glycerol solution of boric acid shows the lowest thermal stability. Structural decomposition at 400 °C occurred without formation of secondary boric acid. The absorption peaks at wavenumber 1390 cm<sup>-1</sup>, 1080–990 cm<sup>-1</sup>, 770 cm<sup>-1</sup> (Fig. 2(c)) were observed after pyrolysis at 800 °C. These absorption bands occurred due to the polymerization of BO<sub>3</sub> and BO<sub>4</sub> groups to diborate and triborate glass structures<sup>[29,30]</sup>. IR studies of PVA/PEG/B<sub>2</sub>O<sub>3</sub> pyrolyzed to 800 °C organic–inorganic precursors prepared by H<sub>3</sub>BO<sub>3</sub> and (CH<sub>3</sub>O)<sub>3</sub>B reveal broad and sharp spectral bands in the different region as shown in Figs. 3(c) and 4(c). Pyrolysis of hybrid PVA/PEG/B<sub>2</sub>O<sub>3</sub> precursors obtained by aqua solution of boric acid and ethanol solution of boron trimethoxide is accompanied with secondary H<sub>3</sub>BO<sub>3</sub> crystallization. The IR spectra show absorptions bands of hydrocarbon residue and BO<sub>3</sub> and BO<sub>4</sub> groups involved in tetraborate glass network (1390 cm<sup>-1</sup>, 1240 cm<sup>-1</sup>, 1100–950 cm<sup>-1</sup>, 695 cm<sup>-1</sup>). The final product is an amorphous carbon/borate glass nanocomposite. Structural changes after pyrolysis investigated by FTIR show that BO<sub>4</sub> structural units are produced only by precursors containing PEG. The presence of BO<sub>4</sub> tetrahedra in the structure without metal counterion can be attendant on electron deficit nature of boron, which takes part in redistributions of π electrons of carbohydrate residues<sup>[13,14]</sup>.

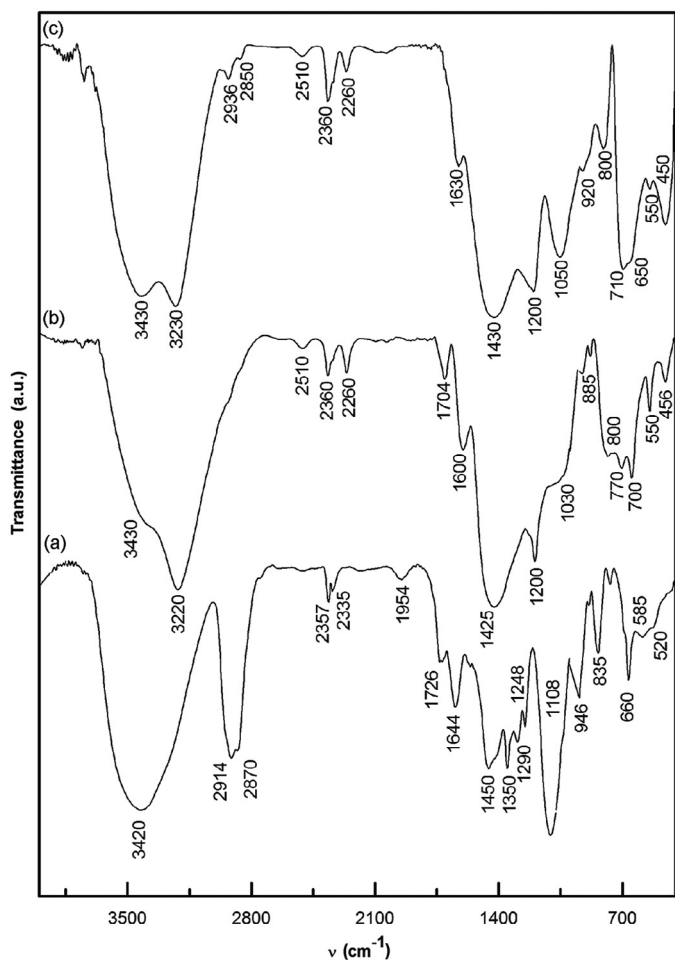


**Fig. 4.** Fourier transform infrared (FTIR) spectra (spectra are vertically shifted) of pyrolyzed PVA/PEG/B<sub>2</sub>O<sub>3</sub> hybrid precursor, prepared from ethanol solution of (CH<sub>3</sub>O)<sub>3</sub>B: (a) 100 °C, (b) 400 °C, (c) 800 °C.

### 3.2. Differential thermal analysis

Differential thermal analysis (DTA) technique was used for thermal characterization of the PVA/PEG/B<sub>2</sub>O<sub>3</sub> precursor obtained by ethanol solutions of (CH<sub>3</sub>O)<sub>3</sub>B. The extent of the degradation process is usually estimated from measurements of mass losses (TGA). Thus, the evaluation of the effect of crosslinking on the degradation behavior of the hybrid materials was performed by measuring the mass loss of samples. The TG/DTA curves are given in Fig. 5(a,b).

In interval of 70–350 °C, the hybrid precursor has lost 55% of its weight. The particular weight loss is between 220 and 350 °C, followed by a further weight loss from 350 to 480 °C. The thermal degradation after 500 °C would not influence the weight losses obviously. Other authors have observed a similar tendency<sup>[20,34,35]</sup>. The most profound endothermic effect at 123 °C can be assigned to the dehydration of adsorbed water molecules and hydrogen bonded cross-linked groups. The next endothermic peak, which appears at 320 °C seems to indicate decomposition of the hybrid structure. The pyrolysis processes can be associated with elimination and scission type reactions of polymer terminal groups, obtaining volatile byproducts, such as water, acetic acid, saturated and unsaturated aldehydes as well as ketones. The appearance of exothermic effects at 387 °C and 670 °C can be explained by steppe mechanism starting with dehydration of H<sub>3</sub>BO<sub>3</sub> and transformations to the metaboric

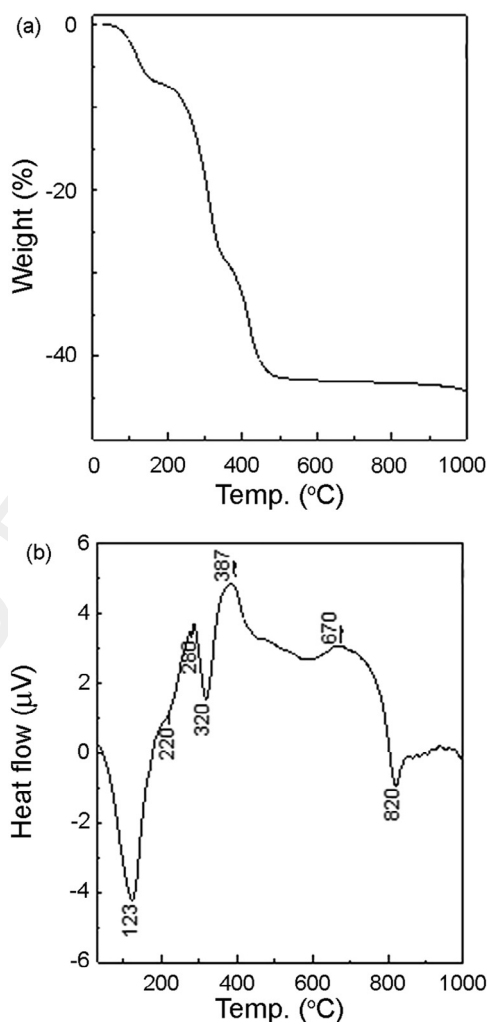


**Fig. 5.** Thermal analyses of PVA/PEG/B<sub>2</sub>O<sub>3</sub> hybrid precursor, prepared from ethanol solution of (CH<sub>3</sub>O)<sub>3</sub>B: (a) TG curve, (b) DTA curve.

(HBO<sub>2</sub>), followed by the tetraboric acid (H<sub>2</sub>B<sub>4</sub>O<sub>7</sub>). The endothermic effect can be observed at 820 °C for the melted boron oxide (B<sub>2</sub>O<sub>3</sub>)<sup>[20,34]</sup>. The XRD results, presented in Fig. 6(a–c) confirm that PVA/PEG/B<sub>2</sub>O<sub>3</sub> precursor is amorphous at 100 °C. Then, the crystallization of boric acid can be observed at 400–700 °C. After that, at 800 °C, the sample is converted to the amorphous molten material.

The presence of carbon nanoparticles may explain the visible changes of the sample in black glass composite<sup>[36]</sup>. The results by SEM are given in Fig. 7. The surface of hybrid films at 100 °C is homogeneous, amorphous without microcracks. The sample at 400 °C consists of particles with a size of 0.1–0.7 μm and their microaggregates are about 1.5 μm. The decrease of particles size and agglomeration can be observed at 800 °C.

### 3.3. Cluster analyses

The data set subjecting to hierarchical cluster analysis had dimension of 12 × 14, where the objects of the study were twelve IR frequencies, which describe 14 different experimental composites. The Ward's method was used for linkage after applying squared Euclidean distance as similarity measure. The cluster significance was determined by the Sneath's index (1/3 and 2/3D<sub>max</sub>). The hierarchical dendrogram is presented, showing the clustering of the composites in Fig. 8. Fourteen different experimental composites

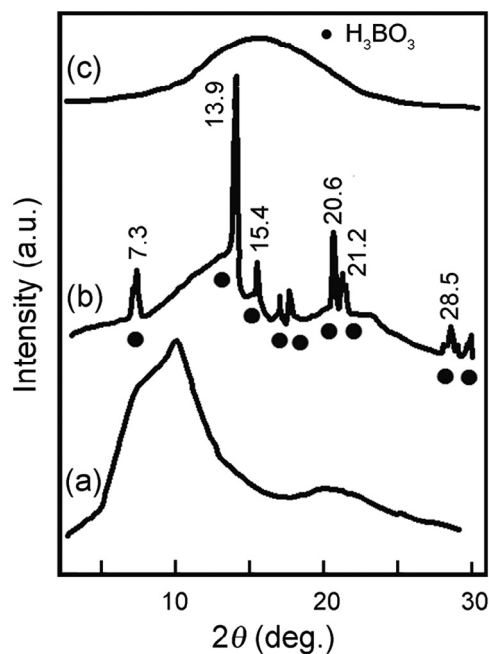


Fig. 6. XRD of PVA/PEG/B<sub>2</sub>O<sub>3</sub> hybrid precursor, prepared from ethanol solution of (CH<sub>3</sub>O)<sub>3</sub>B: (a) 100 °C, (b) 600 °C, (c) 800 °C.

are labeled in the dendrogram and also in the text with the abbreviations. Here is the list of abbreviations in the same order as that in the dendrogram: PB400 and PB800 (binary system PVA/B<sub>2</sub>O<sub>3</sub> pyrolyzed at 400 and 800 °C); PPB(aq.)800, PPB(aq.)25, PPB(aq.)100, PPB(aq.)400 (aqua solution of H<sub>3</sub>BO<sub>3</sub> pyrolyzed at 800 °C, 25 °C, 100 °C, 400 °C); PPB(et.)400, PPB(et.)25, PPB(et.)100, PPB(et.)800 (ethanol solution of trimethyl borate (CH<sub>3</sub>O)<sub>3</sub>B) pyrolyzed at 400 °C, 25 °C, 100 °C, 800 °C); PPB(gl.)25, PPB(gl.)100, PPB(gl.)400, PPB(gl.)800 (glycerol solutions of H<sub>3</sub>BO<sub>3</sub> pyrolyzed at 25 °C, 100 °C, 400 °C, and 800 °C).

Four major clusters could be identified. The first one includes composites synthesized at temperature interval 25–100 °C for three types of hybrids for the system PVA/PEG/B<sub>2</sub>O<sub>3</sub>. This clustering confirms the conclusions that the thermal stability of the composites up to 100 °C does not depend on the initial hybrid structure or the type of the precursor solutions used. The other three groups refer to products pyrolyzed at 400 and 800 °C.

Among the rest of the groups, the linkage including PPB-gl objects (PPB(gl) 25 and PPB(gl) 100) is well defined. Here the similarity is related to the system composition and specificity—the lowest thermal stability is found exactly for this composite structure. At 400 °C it is completely degraded, and the inorganic components are represented by groups BO<sub>3</sub> and BO<sub>4</sub>, which is kept even at 800 °C in a structure of transparent diborate glass.

The linkage for compositions PPB-aq and PPB-et (at 400 and 800 °C) is assumed to be due to the similarity in the thermal aspect, which does not follow the composition similarity. The thermal stability is a function of the hybrid structure type. Due to its lower thermal stability, the hybrid structure of PPB-et at 400 °C reveals much stronger degradation. The reason seems to be the structural dependence on the type of borate solutions; the cross-linking mechanism has to be different. In the same way, the respective B–O structural groups included in the glass nanocomposite (PPB-aq at 800 °C) are present in the powder composition obtained from PPB-et at 400 °C. The last group of linkage for PB-aq (at 400 and 800 °C) concerns proposed hybrid structures obtained by cross-linking of water solutions of PVA and H<sub>3</sub>BO<sub>3</sub>. The thermal behavior is related to the system composition. After pyrolysis at 400 °C, only BO<sub>3</sub>

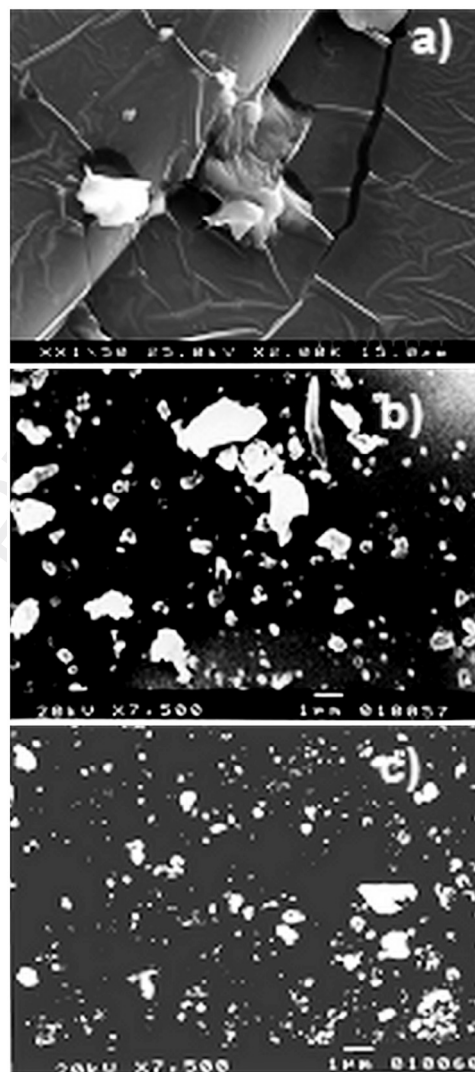


Fig. 7. SEM images of PVA/PEG/B<sub>2</sub>O<sub>3</sub> hybrid precursor, prepared from ethanol solution of (CH<sub>3</sub>O)<sub>3</sub>B: (a) 100 °C, (b) 400 °C, (c) 800 °C.

structural groups are present to be the only structural units of the transparency at 800 °C glass. The different location of this linkage (an outlier) is due to the different composition of the system.

#### 4. Conclusions

The focus of this work is preparation of PVA/PEG/B<sub>2</sub>O<sub>3</sub> precursors for boron doped carbon materials. The quantities and order of borate structural units, residual carbon in networks depend on boron precursor type. After pyrolysis, BO<sub>3</sub> and BO<sub>4</sub> structural groups were obtained in the molten materials like glass or nanocomposite, based on the kind of implementation of boron precursor solution. Glass structures involving polymerized BO<sub>3</sub> and BO<sub>4</sub> groups can be formed in the simultaneous presence of PVA and PEG only. To access the impact of the experimental conditions on the structural changes after pyrolysis of the nanocomposites, cluster analysis of the IR-spectral data was used successfully as the proper classification method.

The clustering reveals new aspects of interpretation of results for boron containing hybrid nanocomposite systems by creating groups of similarity between the organic-inorganic materials independent on specific experimental conditions, which could serve as “fingerprints” for a particular type or nanocomposite.

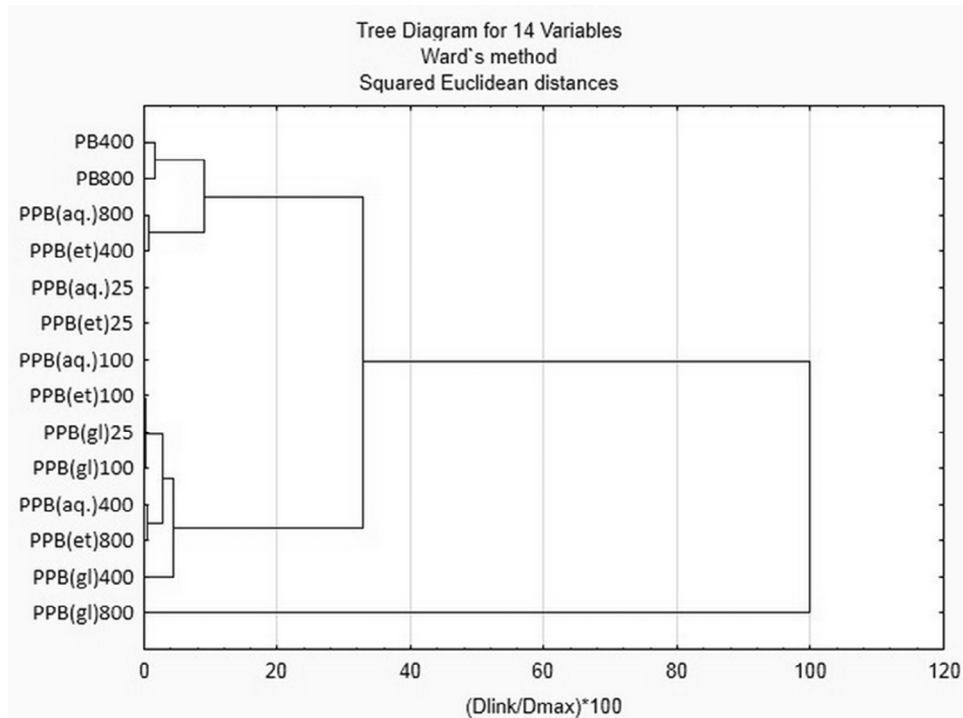


Fig. 8. Hierarchical dendrogram for 14 different experimental composites.

## Acknowledgments

This work was supported by the Spanish Ministry of Education and Science (Project CTM2012-39183) and the Generalitat de Catalunya (Grup Consolidat 2014SGR1017).

## Uncited references

[37], [38]

## References

- [1] C.W. Lepry, S.N. Nazhat, *Chem. Mater.* 27 (2015) 4821–4831. 409
- [2] A. Chandra, A. Bhatt, A. Chandra, *J. Mater. Sci. Technol.* 29 (2013) 193–208. 410
- [3] H. Doweidar, Y.M. Moustafa, G.M. El-Damrawi, R.M. Ramadan, *J. Phys. Condens. Matter* 20 (2008) 369–374. 411
- [4] F. Margha1, A. Abdelghany, *Process. Appl. Ceram.* 6 (2012) 183–192. 412
- [5] P. Pennarun, P. Jannasch, S. Papaefthimiou, N. Skarpentzos, P. Yianoulis, *Thin Solid Films* 514 (2006) 258–266. 413
- [6] Z. Xue, D. He, X. Xie, *J. Mater. Chem. A* 3 (2015) 19218–19253. 414
- [7] C. Chiappe, F. Signori, G. Valentini, L. Marchetti, C. Pomelli, F. Bellina, *J. Phys. Chem. B* 114 (2010) 5082–5088. 415
- [8] J. Luo, C.H. Pardin, X. Zhu, W. Lubell, *J. Comb. Chem.* 9 (2007) 582–591. 416
- [9] B. Pappin, M. Kiefel, T. Houston, C.-F. Chang (Ed.), *Carbohydrates—Comprehensive Studies on Glycobiology and Glycotechnology*, 2012, pp. 37–54. 417
- [10] H. Costa, A. Mansur, M. Pereira, H. Mansur, *J. Nanomater.* 2012 (2012) 1–16. 418
- [11] S. Morris, T. Hawkins, P. Foy, J. Ballato, S.W. Martin, R. Rice, *Int. J. Appl. Glass Sci.* 3 (2012) 144–153. 419
- [12] Y. Lee, H. Joob, L. Radovica, *Carbon* 41 (2003) 2591–2600. 420
- [13] R. Siqueira, I. Yoshida, L. Pardini, M. Schiavon, *Mater. Res.* 10 (2007) 147–151. 421
- [14] S. Labruquère, H. Blanchard, R. Pailler, R. Naslain, *J. Eur. Ceram. Soc.* 22 (2002) 1001–1009. 422
- [15] S. Labruquère, H. Blanchard, R. Pailler, R. Naslain, *J. Eur. Ceram. Soc.* 22 (2002) 1011–1021. 423
- [16] I. Uslu, H. Daştan, A. Altaş, A. Yayli, O. Atakol, M.L. Aksu, *e-Polymers* 7 (2007) 1568–1573. 424
- [17] S. Mondal, A. Banthia, *J. Europ. Ceram. Soc.* 25 (2005) 287–291. 425
- [18] A. Fathi, N. Ehsani, M. Rashidzadeh, H. Baharvandi, A. Rahimnejad, *Ceramics-Silikáty* 56 (2012) 32–35. 426
- [19] I. Uslu, T. Tunc, *J. Inorg. Organomet. Polym.* 22 (2012) 183–189. 427
- [20] P. Barrosa, I. Yoshida, M. Schiavon, *J. Non-Cryst. Sol.* 352 (2006) 3444–3450. 428
- [21] M. Das, S. Ghatak, *Bull. Mater. Sci.* 35 (2012) 99–102. 429
- [22] H. Hristov, P. Vasileva, N. Riskov, C. Dushkin, *J. Optoelectr. Adv. Mater.* 11 (2009) 1343–1346. 430
- [23] P. Vasileva, H. Hristov, N. Riskov, C. Dushkin, *Nanosci. Nanotechnol.* 10 (2010) 201–205. 431
- [24] H. Hristov, P. Vasileva, M. Nedialkova, *Nanosci. Nanotechnol.* 12 (2012) 47–51. 432
- [25] D.L. Massart, L. Kaufman, *The Interpretation of Analytical Chemical Data by the Use of Cluster Analysis*, Wiley-Interscience, New York, 1983. 433
- [26] D.L. Massart, B.G.M. Vandeginste, L.M.C. Buydens, D.L. Massart, B.G.M. Vandeginste, L.M.C. Buydens, S. De Jong, P.J. Lewi, J. Smeyers-Verbeke (Eds.), *Science and Technology*, Elsevier, Amsterdam, 1998. 434
- [27] M. Rozenberg, A. Loewenschuss, Y. Marcus, *Spectrochim. Acta [A.]* 54 (1998) 1819–1826. 435
- [28] S. Gunasekaran, R. Arun Balaji, S. Kumaresan, G. Anand, M. Anand, *Int. J. Chem. Technol. Res.* 1 (2009) 1109–1124. 436
- [29] C. Gautam, A. Kumar Yadav, A. Kumar Singh, *ISRN Ceram.* 2012 (2012) 1–17. 437
- [30] G. Padmaja, P. Kistaiah, *J. Phys. Chem. A* 113 (2009) 2397–2404. 438
- [31] C. Liu, F. Ye, R. Xia, L. Zhang, Y. Zhou, Y. Huang, *J. Mater. Sci. Technol.* 29 (2013) 983–988. 439
- [32] B. Stuart, *Infrared Spectroscopy: Fundamentals and Applications*, Wiley, 2004, pp. 1–76. 440
- [33] I. Prosanov, A. Matvienko, *Phys. Solid State* 52 (2010) 2203–2206. 441
- [34] C. Nyambo, E. Kandare, C. Wilkie, *Polym. Degrad. Stabil.* 94 (2009) 513–520. 442
- [35] C. Gervais, F. Babonneau, N. Dallabonna, D. Soraru, *J. Am. Ceram. Soc.* 84 (2001) 2160–2164. 443
- [36] I. Kottegoda, X. Gao, L. Nayanajith, C.H. Manoranthe, J. Wang, J. Wang, H. Liu, Y. Gofer, *J. Mater. Sci. Technol.* 31 (2015) 907–912. 444
- [37] H. Hristov, M. Nedialkova, *Nanosci. Nanotechnol.* 13 (2013) 147–151. 445
- [38] H. Hristov, M. Nedialkova, *Nanosci. Nanotechnol.* 13 (2013) 152–155. 446